Giant Voids in the Hydrothermally Synthesized Microporous Square Pyramidal−Tetrahedral Framework Vanadium Phosphates $[HN(CH_2CH_2)_3NH]K_{1.35}[V_5O_9(PO_4)_2]\cdot xH_2O$ and $Cs_3[V_5O_9(PO_4)_2]\cdot xH_2O$

M. Isaque Khan,[†,⊥] Linda M. Meyer,[‡] Robert C. Haushalter,*[,‡] Allan L. Schweitzer,[‡] Jon Zubieta,*[,†] and James L. Dye[§]

Department of Chemistry, Syracuse University, Syracuse, New York 13244-4100; NEC Research Institute, 4 Independence Way, Princeton, New Jersey 08540; and Department of Chemistry, Michigan State University, East Lansing, Michigan 48824

Received June 6, 1995. Revised Manuscript Received September 21, 1995[⊗]

The use of a novel mixed-valence pentavanadate phosphate cluster as a building block has made possible the low-temperature hydrothermal self-assembly of the new three-dimensional square pyramidal−tetrahedral framework vanadium phosphates $[HN(CH_2CH_2)_3NH]K_{1.35}[V_5O_9(PO_4)_2]\cdot xH_2O$ (**1**) and $Cs_3[V_5O_9(PO_4)_2]\cdot xH_2O$ (**2**), from structurally simple starting materials. These materials possess some of the lowest framework densities and the largest cavities thus far observed in open-framework solid-state materials. The degree of curvature, size, shape, and charge of the mixed valence $\{V_5O_9(PO_4)_2\}$ V(4+/5+) pentameric building block, which resembles a portion of an arc of a circle, favors the formation of very large cavities. Phosphate **1** crystallizes in space group $I\bar{4}3m$ with $a = 26.247(3)$ Å and has very large cubic-shaped cavities that display $\bar{4}3m$ point symmetry, each of which enclose nearly 50 positive charges. These charges are distributed among 12 $HN(CH_2CH_2)_3NH^{2+}$, 32 K^+ cations, and several waters of crystallization. Each cavity, which could contain a sphere of approximately 13.0 Å diameter and which displays an enormous 32-ring at its maximum diameter, communicates via six 16-ring windows to other similar supercages via intervening smaller cavities. Phosphate **2** is built up from the same pentamers as those in **1** but arranged in a different manner in space group $Fd\bar{3}m$ with $a = 32.306(4)$ Å such that one pentamer lies on each of the six faces of a cube. The three-dimensional structure of **2** consists of two types of cavity, larger ones with all six pentamers curved in an outward fashion, with a free diameter along the diagonal of the cubic-shaped cavity of approximately 20 Å and exhibiting a 24-ring diameter, and smaller ones with all six curved to the inside with cavity diagonals of 7.5 Å. The large cavities are interconnected to one another in a manner that is topologically identical to the arrangement of the carbon atoms in diamond. The ion exchange and sorption properties of these two phosphates are also to be presented.

Utilizing the complicated three-dimensional (3-D) architectures of biological and mineralogical structures as models, synthetic chemistry has recently explored the organization of molecular precursors into aggregates and crystalline solid-state structures on length scales well beyond molecular dimensions. Unlike self-assembled monolayers, synthetic polypeptides or organic host−guest complexes capable of molecular recognition, solid-state inorganic chemistry has provided many examples of materials possessing robust crystalline 3-D covalently bonded lattices. Among the most notable and technologically important of these materials are the microporous aluminosilicate zeolites.[1] To generate large internal micropore volumes in these solids, many of these materials are prepared with large organic cations entrained within the inorganic oxide framework that are subsequently removed to generate the voids. The syntheses are usually performed under relatively mild hydrothermal conditions and are confined to lower temperatures (<200 °C) because of the thermal lability of the organic constituent and the tendency of high-temperature reactions to yield dense phases.

While the tetrahedral framework zeolites remain the most important and studied class of microporous solids, recent synthetic efforts have been directed toward the preparation of non-silicate materials with the goal of preparing solids with pore structures of larger dimensionalities or the discovery of unique framework topologies or novel polyhedral connectivities. Oxide examples include aluminophosphates[2] and zinc and beryllium phosphates and arsenates.[3] Very large pores, whose sizes are defined in terms of the number of non-oxygen

† Syracuse University.
‡ NEC Research Institute.
§ Michigan State University.
⊥ Current address: Department of Chemistry, Illinois Institute of Technology, Chicago, IL 60616.
⊗ Abstract published in *Advance ACS Abstracts,* November 1, 1995.

(1) Occelli, M. L.; Robson, H. E. *Zeolite Synthesis*; American Chemical Society: Washington, DC, 1989. Breck, D. W. *Zeolite Molecular Sieves*; Krieger: Malabar, Florida, 1974. Vaughan, D. E. W. In *ZEOLITES: Facts, Figures, Future*; Jacobs, P. A., van Santen, R. A., Eds.; Elsevier: Amsterdam, 1989; pp 95−116. Meier, W. M.; Olson, D. H. *Atlas of Zeolite Structure Types*; Butterworth: London, 1987. Barrer, R. M. *Hydrothermal Chemistry of Zeolites*; Academic Press: New York, 1982.

0897-4756/96/2808-0043$12.00/0 © 1996 American Chemical Society

framework atoms defining the aperture, have been observed in the aluminophosphate AlPO-8[4] (14-ring pore openings) and VPI-5[5] (18-rings). One of the most open structures known was recently reported in the cubic Ga phoshate cloverite which has 20-ring pore openings.[6] While the large voids, chemical stability and size discriminatory sorptive behavior of the exclusively tetrahedral framework zeolites render them very useful, microporous solids containing transition elements could provide novel properties—such as catalytic, photochemical, and magnetic—not previously accessible by using the diamagnetic, closed-shell main-group systems. Subsequently, microporous behavior was extended into a large class of novel octahedral−tetrahedral framework materials characterized in the molybdenum phosphate system[7] as well as in certain titanium silicates.[8] In addition, we have recently discovered a large number of open-framework structures in the oxovanadium phosphate and oxovanadium phosphonate systems, V−O−$(H_{3-n}PO_4)^{n-}$ and V−O−RPO_3^{2-}, respectively.[9] We report here the hydrothermally mediated self-assembly, single-crystal X-ray structures and physical properties of the square pyramidal−tetrahedral framework vanadium phosphates $[HN(CH_2CH_2)_3NH]K_{1.35}[V_5O_9(PO_4)_2]\cdot 2H_2O$ (**1**) and $Cs_3[V_5O_9(PO_4)_2]\cdot 4.5H_2O$ (**2**). These exceedingly complex networks, composed solely of $\{V_5O_9(PO_4)_{4/2}\}$ pentamers, contain some of the largest voids and apertures and the lowest framework metal atom densities observed to date in open-framework solids.

Experimental Section

The reactions were carried out under autogenous pressure in poly(tetrafluoroethylene)-lined stainless steel Parr acid digestion bombs. KVO_3 and $CsVO_3$ were purchased from Cerac Chemicals. Diaminobicyclooctane (DABCO), diethylamine, phenylphosphonic acid, diaminopropane, and H_3PO_4 (85%) were purchased from Aldrich Chemicals. All reagents were used as received without further purification. Thermal gravimetric analyses were performed on a Perkin-Elmer 7 Series thermal analysis system.

Synthesis of $[HN(CH_2CH_2)_3NH]K_{1.35}[V_5O_9(PO_4)_2]\cdot xH_2O$ (1). A mixture of KVO_3, DABCO, Et_2NH, phenylphosphonic acid, H_3PO_4, and H_2O in the mole ratio 1:2:2:0.75:2:100 was heated for 4 days at 170 °C in a 23 mL Parr acid digestion bomb (35% fill volume). After cooling to room temperature and washing with water, dark green-black truncated tetrahedra of **1** were collected in 75% yield as a monophasic material, as determined by powder X-ray diffraction. Thermal gravimetric analysis of **1** showed a weight loss over the temperature range 25−600 °C of 17.4% (calcd for H_2O + DABCO: 20.7%). The discrepancy between observed and calculated weight loss may be due to water loss from the sample on standing. The calculated value reflects the presence of $2.0H_2O$ of crystallization, which are present in freshly prepared samples of **1**. However, upon standing, the compound does lose water over time if stored in the absence of the mother liquor. For samples carefully stored in the mother liquor, the discrepancy in the weight loss is attributed to the formation upon heating of carbonaceous material which is trapped upon the collapse of the lattice. Samples of **1** decompose in the 425−450 °C range to give a yellow-green glass of unknown identity. IR (KB pellet, cm^{-1}) ν(N−H), 3300−3500; ν(P═O), 1000−1100.

Table 1. Summary of Crystallographic Data for the Structures of $[HN(CH_2CH_2)_3NH]K_{1.35}[V_5O_9(PO_4)_2]\cdot xH_2O$ (1) and $Cs_3[V_5O_9(PO_4)_2]\cdot 4.5H_2O$ (2)

	1	2
formula	$C_6H_{20}K_{1.35}N_2O_{19}P_2V_5$	$Cs_3H_9O_{21.5}P_2V_5$
fw	809.7	1068.5
space group	$I\bar{4}3m$	$Fd\bar{3}m$
a, Å	26.247(3)	32.306(4)
V, Å^3	18082(4)	33719(7)
Z	24	48
D_{calc}, g cm^{-3}	1.784	2.525
μ, cm^{-1}	18.74	56.17
T, K	294	294
radiation	Mo Kα (graphite monochromated, λ = 0.710 73 Å)	
no. of reflections used ($I_o \geq 3\sigma(I_o)$)	875	788
R^a	0.062	0.056
R_w^b	0.068	0.066

^{a} $R = \sum||F_o| - |F_c||/\sum|F_o|$. ^{b} $R_w = [\sum w(|F_o| - |F_c|)^2/\sum w(|F_o|)^2]^{1/2}$.

Synthesis of $Cs_3[V_5O_9(PO_4)_2]\cdot 4.5H_2O$ (2). A mixture of Cs_3VO_3, 1,3-diaminopropane, H_3PO_4 and H_2O in the mole ratio 3:5:5:2000 was heated for 2 days at 200 °C in a 23 mL Parr acid digestion bomb (45% fill volume). After cooling to room temperature and washing with water, green-black cubes of **2** were isolated in 20% yield based on vanadium. Thermal gravimetric analysis of **2** is consistent with loss of all water of crystallization between 90 and 110 °C.

X-ray Crystallography. X-ray data were collected on a Rigaku AFC7R diffractometer with graphite monochromated Mo Kα radiation and a 18 kW rotating anode generator. The crystal dimensions of **1** and **2** (0.15 × 0.10 × 0.08 mm and 0.11 × 0.09 × 0.12 mm, respectively) and weak diffraction profiles necessitated the use of the rotating anode system. The structures were solved by direct methods; both were refined by full-matrix least-squares using SHELXS-86, SHELXTL or TEXSAN program packages.[10−13] In both cases, refinement proceeded routinely, and no anomalies in temperature factors or excursions of electron density in the final Fourier maps were observed.

Table 1 summarizes the crystal parameters and details of the structure solutions and refinements. Atomic positional parameters for **1** and **2** are given in Tables 2 and 3, respectively. Selected bond lengths and angles for **1** and **2** are listed in Tables 4 and 5, respectively.

(2) Szostak, R. *Molecular Sieves Principles of Synthesis and Identification*; Van Nostrand Reinhold: New York, 1989. Meier, W. M.; Olson, D. H. *Atlas of Zeolite Structure Types*; Butterworth: London, 1987. Occelli, M. L.; Robson, H. E. *Zeolite Synthesis*; American Chemical Society: Washington, D.C., 1989; Chapter 23.
(3) Gier, T. E.; Stucky, G. D. *Nature* **1991**, *349*, 508.
(4) Dessau, R. M.; Shirker, J. L.; Higgins, J. B. *Zeolites* **1990**, *10*, 522.
(5) Davis, M. E.; Saldarriaga; Montes, C.; Garces, J.; Crowder, C. *Nature* **1988**, *331*, 698.
(6) Estermann, M.; McKusker, L. B.; Baerlocher, C.; Merrouche, A.; Kessler, H. *Nature* **1991**, *352*, 320.
(7) Haushalter, R. C.; Mundi, L. A. *Chem. Mater.* **1992**, *4*, 31.
(8) (a) Kuznicki, S. M.; Thrush, K. A.; Allen, F. M.; Levine, S. M.; Kamil, M. M.; Hayhurst, D. T.; Mansour, M. *Synth. Microporous Mater.* **1992**, *1*, 427. (b) Poojary, D. M.; Cahill, R. A.; Clearfield, A. *Chem. Mater.* **1994**, *6*, 2364. (c) U.S. Patent 4853202; European Patent Appl. 0405978 A1.
(9) Soghomonian, V.; Chen, Q.; Haushalter, R. C.; Zubieta, J. *Angew. Chem., Int. Ed. Engl.* **1995**, *34*, 223. Soghomonian, V.; Haushalter, R. C.; Chen, Q.; Zubieta, J. *Inorg. Chem.* **1994**, *33*, 1700. Soghomonian, V.; Haushalter, R. C.; Chen, Q.; Zubieta, J. *Science* **1993**, *256*, 1596. Soghomonian, V.; Haushalter, R. C.; Chen, Q.; Zubieta, J. *Angew. Chem., Int. Ed. Engl.* **1993**, *32*, 610. Soghomonian, V.; Haushalter, R. C.; Chen, Q.; Zubieta, J. *Chem. Mater.* **1993**, *5*, 1690. Soghomonian, V.; Haushalter, R. C.; Chen, Q.; Zubieta, J. *Chem. Mater.* **1993**, *5*, 1595.
(10) Calabrese, J. C. PHASE-Patterson Heavy Atom Solution Extractor; University of Wisconsin—Madison, Ph.D. Thesis, 1972. Beurskens, P. T. DIRDIF-Direct Methods for Difference Structures and Automatic Procedure for Phase Extraction and Refinement of Difference Structure Factors. Thechnical Report 1984/1, Crystallographic Laboratory, Toernooiveld, 6525 Ed Nijmegen, Netherlands.
(11) Cromer, D. T.; Waber, J. T. *International Tables for X-ray Crystallography*; Kynoch Press: Birmingham, England, 1974; Vol. IV, Table 2.2A.
(12) Ibers, J. A.; Hamilton, W. C. *Acta Crystallogr.* **1964**, *17*, 781.
(13) Cromer, D. T. *International Tables for X-ray Crystallography*; Kynoch Press: Birmingham, England, 1974; Vol. IV, Table 2.3.1.

Table 2. Atomic Positional Parameters ($\times 10^4$) and Isotropic Temperature Factors ($Å^2 \times 10^3$) for $[H_2DABCO]K_{1.35}[V_5O_9(PO_4)_2]\cdot xH_2O$ (1)

	x	*y*	*z*	*U*(eq)[a]
V(1)	6982(2)	−1227(2)	6982(2)	31(2)
V(2)	7523(2)	−411(2)	7523(2)	34(2)
V(3)	7276(2)	650(2)	7276(2)	30(2)
V(4)	6506(2)	303(2)	2067(2)	35(2)
K(1)	2176(3)	2176(3)	2176(3)	47(2)
K(2)	6755(4)	1642(3)	1642(3)	56(4)
K(3)	5000	−2500	10000	90(9)
P(1)	6127(3)	−835(3)	2345(3)	39(3)
O(1)	7560(6)	1057(8)	7560(6)	42(7)
O(2)	6551(6)	−858(6)	2728(6)	48(5)
O(3)	7102(5)	−120(5)	2237(5)	33(4)
O(4)	7961(7)	−533(9)	7961(7)	60(8)
O(5)	6948(5)	815(5)	2382(5)	21(4)
O(6)	5906(6)	628(6)	2382(6)	49(5)
O(7)	6520(7)	470(6)	1485(7)	58(5)
O(8)	6099(6)	−318(6)	2074(6)	45(5)
O(9)	7161(7)	−1771(9)	7161(7)	54(7)
O(10)	6921(6)	1204(6)	3759(6)	49(5)
O(11)	1610(13)	1610(13)	1610(13)	117(21)
O(12)	0	0	3543(21)	133(20)
O(13)	7691(20)	1368(14)	1368(14)	219(23)
O(14)	3132(30)	3132(30)	3132(30)	268(66)
O(15)	6670(14)	6670(14)	−134(19)	69(17)
O(16)	5627(26)	1125(17)	1125(17)	109(23)
N(1)	2187(20)	1021(13)	1021(13)	165(21)
N(2)	2926(20)	510(14)	510(14)	163(20)
C(1)	2147(14)	475(12)	1184(14)	107(13)
C(2)	2747(18)	1177(14)	1177(14)	143(23)
C(3)	2587(17)	156(17)	908(17)	177(23)
C(4)	3173(20)	897(14)	897(14)	175(31)

[a] Equivalent isotropic *U* defined as one-third of the trace of the orthogonalized U_{ij} tensor.

Table 3. Atomic Positional Parameters ($\times 10^4$) and Isotropic Temperature Factors ($Å^2 \times 10^3$) for $Cs_3[V_5O_9(PO_4)_2]\cdot 4.5H_2O$ (2)

	x	*y*	*z*	*U*(eq)[a]
Cs(1)	92(1)	92(1)	1263(1)	62(1)
Cs(2)	1910(1)	1910(1)	−2144(1)	65(1)
V(1)	−686(1)	−686(1)	−9143(1)	20(1)
V(2)	8750	2050(1)	3750	11(1)
V(3)	3175(1)	3175(1)	−3346(1)	11(1)
P(1)	0	1250	8750	10(1)
O(1)	435(3)	435(3)	−514(5)	21(4)
O(2)	44(6)	1250	1250	24(5)
O(3)	425(3)	425(3)	2997(4)	23(4)
O(4)	709(2)	−654(2)	−8742(3)	9(2)
O(5)	−267(2)	−856(2)	−8736(4)	16(3)
O(6)	273(2)	−12167(4)	−8361(3)	17(3)
O(7)	1250	1250	−1468(10)	65(9)
O(8)	2437(12)	2437(12)	6108(17)	112(20)
O(9)	−1767(10)	−1767(10)	−1767(10)	137(21)
O(10)	1842(14)	852(14)	−2100(15)	56(16)
O(11)	−478(12)	−478(12)	−478(12)	53(19)
O(12)	−879(16)	−879(16)	−879(16)	96(30)
O(13)	2758(11)	2758(11)	2758(11)	40(16)

[a] Equivalent isotropic *U* defined as one-third of the trace of the orthogonalized U_{ij} tensor.

Adsorption Measurements. Water vapor absorption isotherms were recorded on a Micrometrics ASAP 2010 (accelerated surface area and porosity). The samples were degassed under vacuum at 50 °C until the sample degas rate was constant for 5 min. The sample was then submerged in an ice bath and exposed to water vapor which was introduced quantitatively. When the pressure of the sample equilibrated, this pressure was recorded. For this study, water was introduced in quantities of 2.00 cm^3/g at STP. Equilibration times ranged from a minimum of 0.75 h to a maximum of 1.00 h. Samples of 0.1010 and 0.0804 g were used in the measurements of the isotherms of **1** and **2**, respectively.

Table 4. Selected Bond Lengths (Å) and Angles (deg) for $[H_2DABCO]K_{1.35}[V_5O_9(PO_4)_2]\cdot xH_2O$ (1)

	Apical Vanadium Site[a]		
V(2)−O(4)[b]	1.66(3)	O(3)−V(2)−O(3a)	81.1(8)
V(2)−O(3)	1.89(1) (×2)[c]	O(3)−V(2)−O(5)	84.3(6)
V(2)−O(5)	1.86(1) (×2)	O(3)−V(2)−O(5a)	140.2(7)
		O(5)−V(2)−O(5a)	83.8(9)
		O(4)−V(2)−O(3)	108.6(7)
		O(4)−V(2)−O(5)	111.1(7)
	Basal Vanadium Sites		
V(1)−O(9)	1.58(2)	O(5)−V(1)−O(5a)	77.4(8)
V(1)−O(5)	1.99(1) (×2)	O(5)−V(1)−O(10)	90.4(6)
V(1)−O(10)	1.95(2) (×2)	O(5)−V(1)−O(10a)	144.5(7)
		O(10)−V(1)−O(10a)	80.5(10)
		O(9)−V(1)−O(5)	104.8(8)
		O(9)−V(1)−O(10)	110.5(8)
V(3)−O(1)	1.50(2)	O(2)−V(3)−O(2a)	85.1(10)
V(3)−O(2)	1.98(2) (×2)	O(2)−V(3)−O(3)	88.6(6)
V(3)−O(3)	1.94(2) (×2)	O(3)−V(3)−O(3a)	146.0(7)
		O(3)−V(3)−O(3a)	78.3(8)
		O(1)−V(3)−O(2)	106.5(8)
		O(1)−V(3)−O(3)	107.4(8)
V(4)−O(7)	1.59(2)	O(7)−V(4)−O(3)	110.8(8)
V(4)−O(3)	1.97(1)	O(7)−V(4)−V(5)	101.7(8)
V(4)−O(5)	1.96(1)	O(7)−V(4)−O(6)	107.6(8)
V(4)−O(6)	1.97(1)	O(7)−V(4)−O(8)	104.6(8)
V(4)−O(8)	1.95(1)	O(3)−V(4)−O(5)	79.7(6)
		O(3)−V(4)−O(6)	141.5(7)
		O(3)−V(4)−O(8)	87.8(6)
		O(5)−V(4)−O(6)	90.0(6)
		O(5)−V(4)−O(8)	153.5(7)
		O(6)−V(4)−O(8)	85.4(7)
	Phosphate Groups		
P(1)−O(2)	1.50(2)	O(2)−P(1)−O(6)	112.3(6)
P(1)−O(6)	1.51(2)	O(2)−P(1)−O(8)	108.7(10)
P(1)−O(8)	1.54(2)	O(2)−P(1)−O(10)	110.9(10)
P(1)−O(10)	1.55(2)	O(6)−P(1)−O(8)	106.8(9)
		O(6)−P(1)−O(10)	111.7(10)
		O(8)−P(1)−V(10)	106.3(9)
	Potassium Sites		
K(1)−O(1)	3.10(2) (×3)	K(2)−O(5)	2.96(1)
K(1)−O(9)	2.77(2) (×3)	K(2)−O(7)	3.17(2) (×2)
		K(2)−O(2)	2.89(2) (×2)
		K(2)−O(9)	3.33(2) (×2)
K(3)−O(6)	2.91(2) (×4)		
K(3)−O(8)	3.20(2) (×4)		
	Vanadium−Vanadium Distances		
V(2)−V(1)	2.937(8)		
V(2)−V(3)	2.932(8)		
V(2)−V(4)	2.893(5)		

[a] The unique V site in **1** is V(2); this apical site is labeled V_a in Table 6. V(1), V(3), and V(4) are basal vanadium sites, V_b. [b] The simplified labelling scheme adopted for oxygen atoms in Table 6 adopts the following notation: O(1), O(4), O(7), and O(9) are terminal oxo groups, O_t. O(3) and O(5) are bridging oxo groups, O_b. O(2), O(6), O(8), and O(10) are phosphate oxygen atoms, O(phosphate). [c] The notation $\times N$ (N = an integer) refers to the number of symmetry-equivalent oxygen atoms bonded to the metal site.

Results and Discussion

Hydrothermal synthesis has been demonstrated to provide a low-temperature pathway to metastable structures utilizing inorganic and organic molecular units of a desired geometry while allowing the introduction of a variety of inorganic and/or organic cations as templates for the organization of the networks of oxovanadium polyhedra and phosphorus tetrahedra.[9] However, it has become clear that the identity of the product isolated is critically dependent on reaction conditions and that the parameter space associated with the hydrothermal technique is vast, with factors such as temperature, stoichiometries, pH, fill volume, surface nucleation,

Table 5. Selected Bond Lengths (Å) and Angles (deg) for $Cs_3[V_5O_9(PO_4)_2]\cdot 4.5H_2O$ (2)

		Apical Vanadium Site[a]	
V(2)−O(2)[b]	1.60(2)	O(2)−V(2)−O(4)	109.8(3)
V(2)−O(4)	1.86(7) (×4)[c]	O(4)−V(2)−O(4a)	140.4(5)
		O(4)−V(2)−O(4b)	84.9(6)
		Basal Vanadium Sites	
V(1)−O(1)	1.60(2)	O(1)−V(1)−O(4)	104.7(5)
V(1)−O(4)	1.97(10) (×6)	O(1)−V(1)−O(5)	104.8(5)
V(1)−O(5)	1.96(10) (×6)	O(4)−V(1)−O(4a)	78.9(4)
		O(4)−V(1)−O(5)	150.2(4)
		O(4)−V(1)−O(5a)	89.9(3)
		O(5)−V(1)−O(5a)	86.4(6)
V(3)−O(3)	1.61(1)	O(3)−V(3)−O(4)	105.5(5)
V(3)−O(4)	1.95(1) (×2)	O(3)−V(3)−O(6)	107.9(5)
V(3)−O(6)	1.97(1) (×2)	O(4)−V(3)−O(4a)	77.4(4)
		O(4)−V(3)−O(6)	146.3(4)
		O(4)−V(3)−O(6a)	88.9(3)
		O(6)−V(3)−O(6a)	85.8(6)
		Phosphate Group	
P(1)−O(5)	1.54(8) (×2)	O(5)−P(1)−O(5a)	111.4(8)
P(1)−O(6)	1.54(8) (×2)	O(5)−P(1)−O(6)	110.7(4)
		O(5)−P(1)−O(6a)	109.1(6)
		O(6)−P(1)−O(6a)	105.8(8)
		Cesium Sites	
Cs(1)−O(1)	3.50(1) (×2)	Cs(2)−O(3)	3.30(1) (×2)
Cs(1)−O(3)	3.413(9) (×2)	Cs(2)−O(5)	3.15(1) (×2)
Cs(1)−O(4)	3.105(7) (×2)	Cs(2)−O(8)	3.38(4) (×2)
Cs(1)−O(5)	3.276(8) (×2)	Cs(2)−O(10)	3.43(5)
Cs(1)−O(9)	3.35(2)		
Cs(1)−O(11)	3.089(3)		
		Vanadium−Vanadium Distances	
V(2)−V(1)	2.894(4)		
V(2)−V(3)	2.923(4)		

[a] The unique apical vanadium site in **2** is V(2); as for compound **1**, this site is denoted V_a for purposes of comparison in Table 6. V(1) and V(3) are basal sites, V_b. [b] The simplified labeling scheme for oxygen atoms in Table 6 adopts the following notation: O(1), O(2), and O(3) are terminal oxo groups, O_t; O(4) is the bridging oxo group, O_b; O(5) and O(6) are phosphate oxygen atoms, O(phosphate). [c] The notation $\times N$ (N = an integer) refers to the number of symmetry-equivalent oxygen atoms of a given type bonded to the metal site.

nature of the oxometal source, and templating reagents contributing to the chemistry. The structural chemistry of the $V-O-PO_4^{3-}$ system has been demonstrated to be extensive, and suitable modifications in reaction conditions have now been exploited in the synthesis of the supercage phases $[H_2DABCO]K_{1.35}[V_5O_9(PO_4)_2]\cdot xH_2O$ (**1**) and $Cs_3[V_5O_9(PO_4)_2]\cdot 4.5H_2O$ (**2**).

The phosphate $[HN(CH_2CH_2)_3NH]K_{1.35}[V_5O_9(PO_4)_2]\cdot xH_2O$ (**1**) is prepared from the reaction of KVO_3:$N(CH_2CH_2)_3N$:Et_2NH:phenylphosphonic acid:H_3PO_4:H_2O in a molar ratio of 1:2:2:0.75:2:100 for 4 days at 170 °C and is isolated in 75% yield as a single phase of perfectly formed, dark green-black rhombic dodecahedra or truncated tetrahedra. The infrared spectrum of **1** exhibits bands in the 3300−3500 cm^{-1} range associated with ν(N−H) of the $H_2-DABCO^{2+}$ cation and two strong absorptions in the 1000−1100 cm^{-1} region attributed to ν(P═O). A curious feature of the synthesis of **1** is the absolute requirement of the reagents Et_2NH and phenylphosphonic acid for the isolation of **1** as monophasic crystalline material in good yield, although neither appears in the product. This is not an uncommon observation in the hydrothermal synthesis of oxovanadium phosphate phases.[9] The role of the organoamine appears to be adjustment of pH, maintenance of reducing reaction conditions, and deprotonation of the phenylphosphonic acid. This latter reagent may be

Table 6. Comparison of the Structural Parameters for the $\{V_5O_9(PO_4)_{4/2}\}$ Cores of 1 and 2, the $\{V_5O_9(PhPO_3)_{4/2}\}$ Cores of $[\{NH_4Cl\}_2V_{14}O_{22}(OH)_4(H_2O)_2(PhPO_3)_8]^{6-}$ and $[(CH_3CN)_2V_{14}O_{22}(OH)_4(PhPO_3)_8]^{6-}$, and the $\{V_5O_9(RCO_2)_4\}$ Core of $[V_5O_9(thiophene\text{-}2\text{-}carboxylate)_4]^{2-}$

	apical V site (V_a)			basal V sites (V_b)				
	$V{=}O_t$[a]	$V-O_b$	V_a-O-V_b	$V{=}O_t$	$V-O_b$	$V-O_{(ligand)}$	V_b-O-V_b	average V oxidation state
1	1.66(3)	1.88(2)	98.7(6)	1.56(2)	1.97(2)	1.96(2)	137(1)	4.2
2	1.60(1)	1.857(7)	99.3(4)	1.60(1)	1.96(1)	1.97(1)	139.7(4)	4.2
$[\{NH_4Cl\}_2V_{14}O_{22}(OH)_4(H_2O)_2(PhPO_3)_8]^{6-}$	1.600(2)	1.857−1.888(2)	*b*	1.578−1.600(2)	1.951−1.980(2)	*b*	*b*	4.2
$[(CH_3CN)_2V_{14}O_{22}(OH)_4(PhPO_3)_8]^{6-}$	1.60(1)	1.88(1)	99.1(3)	1.57(1)	1.97(1)	1.97(1)	138.6(7)	4.2
$[V_5O_9(RCO_2)_4]^{2-}$	1.597(6)	1.883(7)	*b*	1.591(7)	1.963(7)	2.005−2.033(6)	*b*	4.0

[a] Abbreviation used: $O_t \equiv$ terminal oxo group; $O_b \equiv$ bridging oxo group; O(ligand) ≡ PO_4^{3-}, $PhPO_3^{2-}$, or RCO_2^- "ligand" oxygen. [b] Not reported.

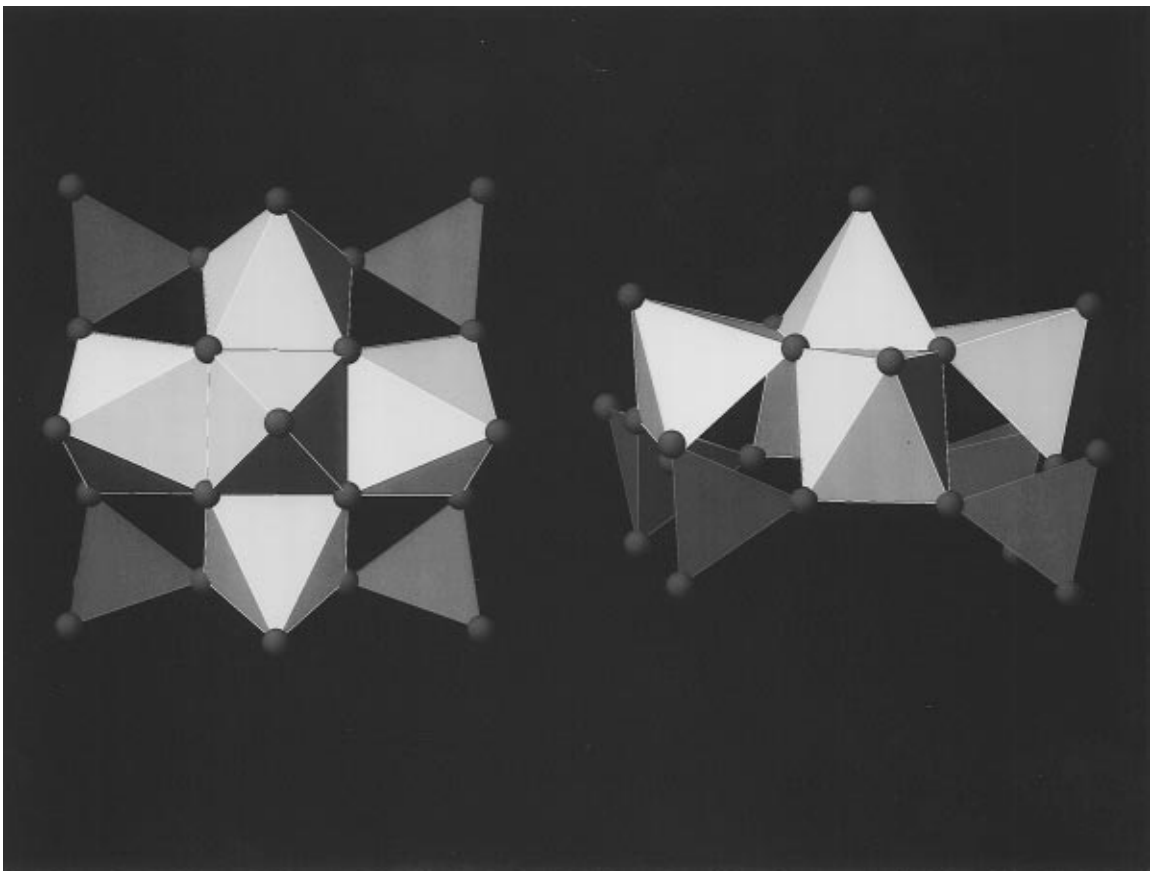

Figure 1. Curved pentameric $\{V_5O_9(PO_4)_{4/2}\}$ units present in phosphates **1**−**3**.

required to provide a repository of V(IV) in cluster form for subsequent reaction with phosphate. The $\{V_5O_9(PO_4)_{4/2}\}$ cluster which provides the fundamental structural motif for the solids of this study (vide infra), finds its counterpart as $\{V_5O_9(RPO_3)_{4/2}\}$ in the molecular clusters of the oxovanadium organophosphonate system, represented by $[XV_{14}O_{22}(OH)_4(H_2O)_2(PhPO_3)_8]^{n-}$ (X = 2 × NH_4Cl, $n = 6$; X = N_3^-, $n = 7$).[14] While it is tempting to speculate that the synthesis of **1** occurs by self-assembly of such molecular precursors, there is no evidence for structural preassembly in this case.

The fundamental building blocks of the framework of **1** are VO_5 square pyramids and PO_4 tetrahedra. All V atoms possess terminal V=O (vanadyl) groups and are present in the form of unusual cross-shaped V_5 pentamers that consist of a central VO_5 square pyramid sharing each of its four basal edges with edges from four additional square-pyramidal vanadium centers as shown in Figure 1. As shown by the comparison of metrical parameters in Table 6, the pentanuclear unit of **1** is closely related to the $\{V_5O_9(PhPO_3)_{4/2}\}$ unit of the molecular clusters $[\{NH_4Cl\}_2V_{14}O_{22}(OH)_4(H_2O)_2(PhPO_3)_8]^{6-}$, and $[(CH_3CN)_2V_{14}O_{22}(OH)_4(PhPO_3)_8]^{6-}$,[15] and to the core structure of $[V_5O_9(\text{thiophene-2-carboxylate})_4]^{2-}$.[16] Each pentamer is connected to four other V_5 units via 4/2 phosphate tetrahedra (Figure 1). Valence sum calcula-tions[17] give a value of 20.7+ for the five V atoms (average = $V^{4.2+}$) yielding a calculated framework charge of $[V_5O_9(PO_4)_2]^{3.3-}$ in good agreement with the −3.35 required if the H_2DABCO^{2+} cations were all fully protonated and the K^+ sites fully occupied.

The most prominent feature of the $I\bar{4}3m$ structure is the extremely large voids in the V−P−O framework, centered about 0, 0, 0 and $^1/_2$, $^1/_2$, $^1/_2$, which have rigorous $\bar{4}3m$ site symmetry and are apparent in the projection of the unit-cell contents down [100] (Figure 2a). These cavities are filled in a remarkably complicated, but highly symmetric, manner with a mixture of organic and inorganic cations. The center of the cavity contains an aggregate of twelve $HN(CH_2CH_2)_3NH^{2+}$ (diprotonated 1,4-diazabicyclooctane = H_2DABCO^{2+}) dications (Figure 3a) that are arranged with the symmetry of a truncated tetrahedron as shown in Figure 3b. One N atom of each H_2DABCO^{2+} lies on each of the 12 vertices of a truncated tetrahedron. These 12 organic moieties are surrounded by 32 K^+ cations present as eight tetramers (Figure 3c). All eight crystallographically equivalent tetramers are arranged in the form of two interpenetrating tetrahedra which yields a tetrahedrally distorted cube with one tetramer on each corner of the cube (Figure 3c). The organic and K^+ cations, and the waters of crystallization, are in turn surrounded by a cavity formed from 12 vanadium pentamers, connected by phosphate groups and corners of other adjacent pentamers, the central V atoms of which also lie at the vertices of a truncated tetrahedron (Figure 3d). Thus for 1.35 K^+ and 1 DABCO per pentamer, there is a total of 40.2 positive charges/cavity, which agrees very well

(14) (a) Müller, A.; Hovemieir, K.; Rohlfing, R. *Angew. Chem., Int. Ed. Engl.* **1992**, *31*, 1192, for the analogous organoarsonates see ref 15. (b) Müller, A.; Hovemieir, K.; Krickemeyer, E.; Bögge, H. *Angew. Chem., Int. Ed. Engl.* **1995**, *34*, 779.

(15) Khan, M. I.; Zubieta, J. *Angew. Chem., Int. Ed. Engl.* **1994**, *33*, 760.

(16) Hunrich, D. D.; Folting, K.; Streib, W. E.; Huffman, J. C.; Chistou, G. *J. Chem. Soc., Chem. Commun.* **1989**, 1411.

(17) Brown, K. D.; Wu, K. K. *Acta Crystallogr.* **1976**, *B32*, 1957.

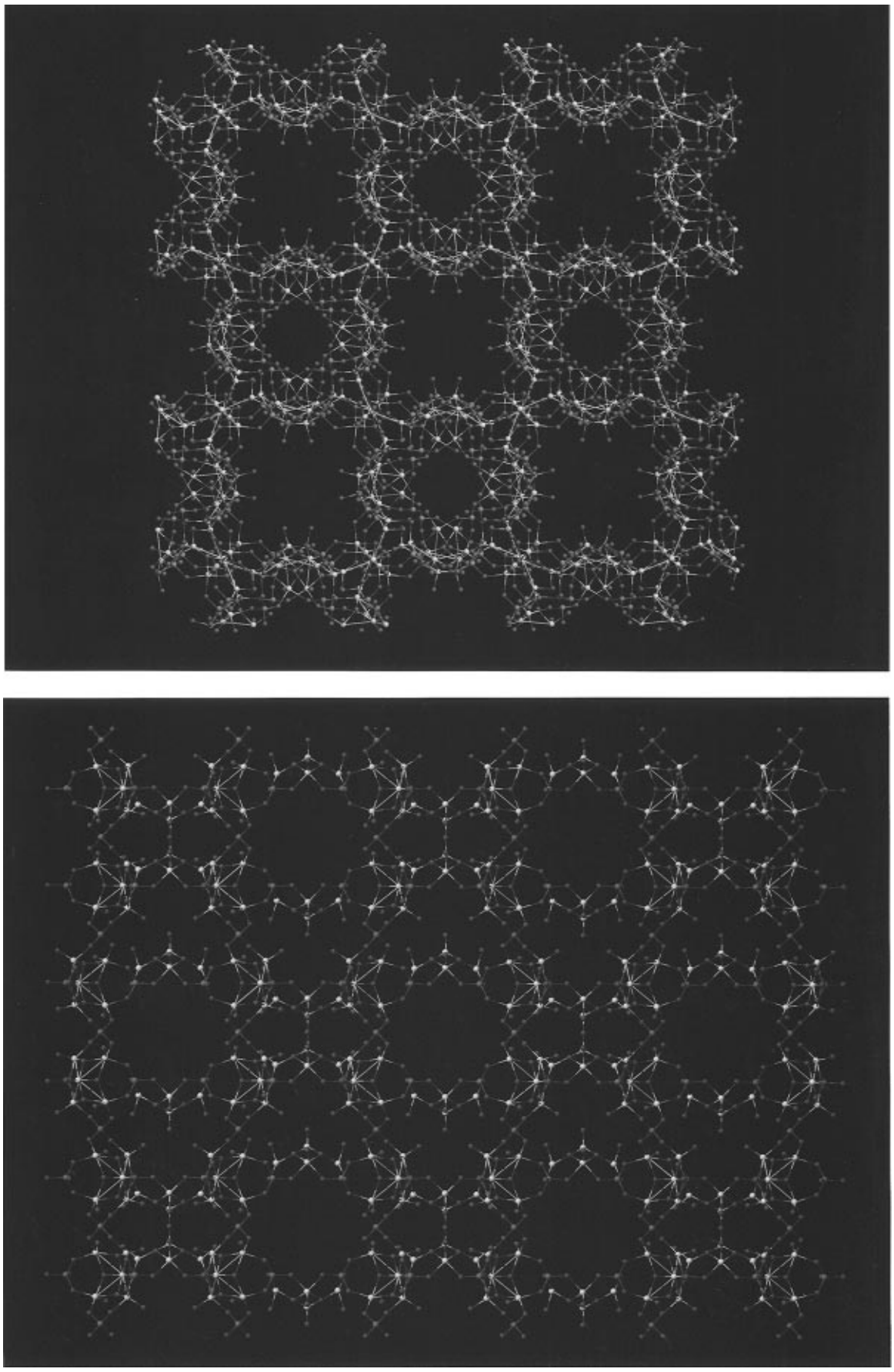

Figure 2. Unit-cell contents of (top) phosphate (**1**) and (bottom) that for (**2**) projected down the [100] and [110] directions, respectively.

with the framework charge requirement of −39.6 from the vanadium valence sum calculations.[17]

As shown in Figure 1, this $\{V_5O_9(PO_4)_{4/2}\}$ unit displays a pronounced bending with various V−V−V

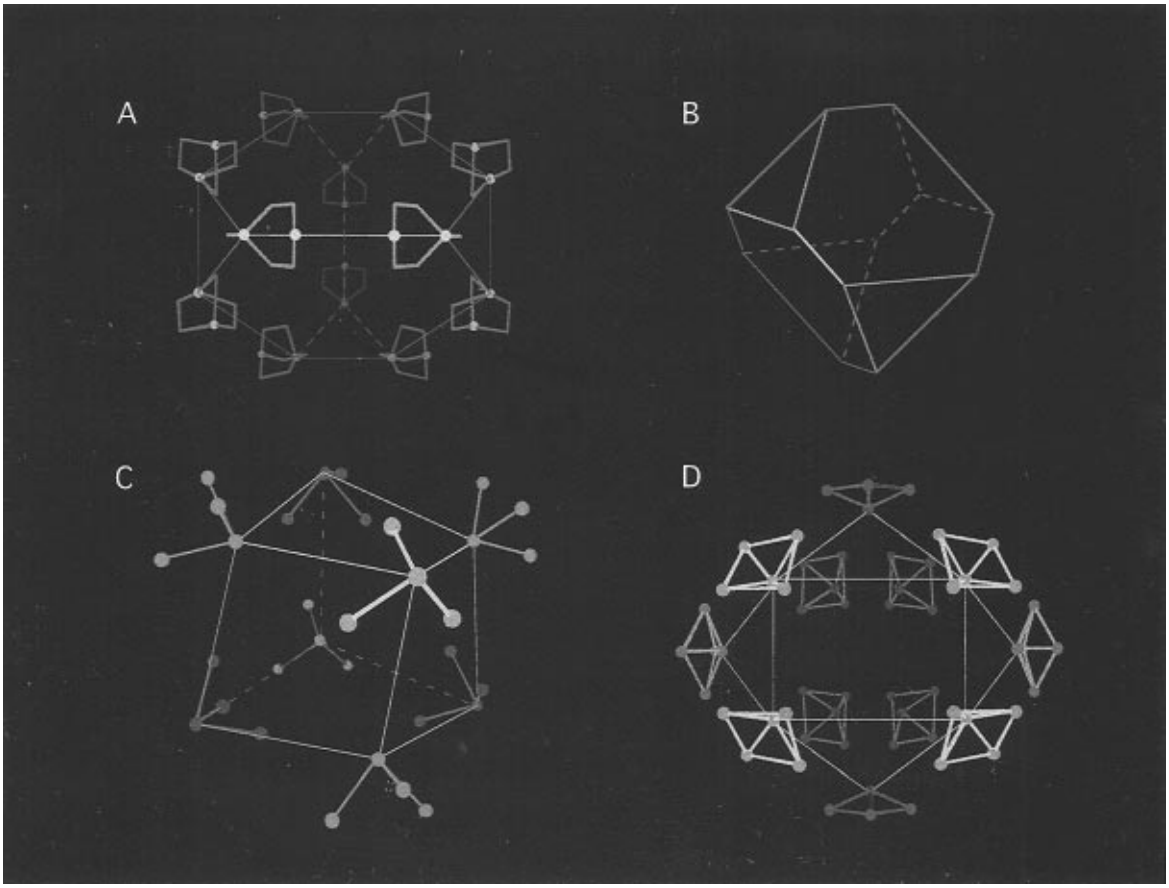

Figure 3. Schematic representation of the contents of the large cavity at 0, 0, 0 ($\bar{4}3m$ point symmetry) in (**1**). The center of the cavity contains (a) 12 $HN(CH_2CH_2)_3NH^{2+}$ (diazabicyclooctane = DABCO) cations. One N atom of each DABCO lies on each of the 12 vertices of a truncated tetrahedron (b). The organic cations are surrounded by a distorted cube of 32 K^+ cations present as eight tetramers (c). All of these cations are enclosed in turn within 12 V_5 pentamers, the central V atoms of which also lie on the vertices of a truncated tetrahedron (d).

angles subtended at the apex of approximately 125° ± 10° in **1** and **2**. The combination of this curvature, the tetrahedral coordination requirements of the P, the distance between the 4/2 PO_4 groups and the relatively low charge per volume in the pentamer, all favor metrically large structures that would have difficulty filling all space in a typically dense fashion. The surprisingly large volume of these voids is reflected in the very low framework metal atom density. For **1**, there are only about 9.3 M atoms (M = V, P)/1000 Å^3 compared with values of about 12.7 and 11.1 atoms/1000 Å^3 for the very open faujasite (M = Si) and cloverite (M = Ga, P), respectively, making **1** among the lowest framework density materials known even when taking into account that the V atoms are five coordinate. A cross sectional view of this cavity (Figure 4) shows the enormous 32-ring present at the maximum diameter of the cavity. To the best of our knowledge, this is the largest contiguous aperture observed thus far in a solid state material.

The interconnection of the large voids generates a fascinating tunnel topology. Each large cavity at 0, 0, 0 has six rectangular 16-ring windows (Figure 5a) that surround the origin in an octahedral fashion, through which it communicates with six other symmetry equivalent voids along ⟨100⟩ via intervening smaller cavities. The 16-ring windows (Figure 5a) have free dimensions (minimum O−O distance less one O radius of 2.6 Å) of about 9.4 by 4.4 Å, while the intervening smaller cavities possess a free diameter of approximately 6.5 Å. These smaller voids, containing 8-ring windows with a K^+ cation loosely centered in each window (Figure 5b), lie on the midpoints of the unit cell edges half way between the large voids. Since the unit cell is body centered, there is a crystallographically equivalent set of voids and tunnels centered about $^1/_2$, $^1/_2$, $^1/_2$. The array of tunnels and voids containing the cavity at the origin interpenetrates, but never intersects, the array containing the cavity at $^1/_2$, $^1/_2$, $^1/_2$ (Figure 6). A naturally occurring zeolite, paulingite,[18] possesses an array of (much smaller) tunnels with a similar topology. The isosurface that lies between the framework atoms and the voids is depicted[19] in Figure 6 where the two interpenetrating but independent and nonintersecting tunnel networks, as well as the interconnection of each large cavity via intervening smaller cavities, are apparent.

According to powder X-ray diffraction measurements, another phosphate, **3**, with a framework isostructural to that found in **1** but with charge-compensating piperidinium cations in place of DABCO, can be prepared as a single phase by substituting piperidine for DABCO in the synthesis.[20]

The vanadium phosphate supercage material $Cs_3[V_5O_9(PO_4)_2]\cdot xH_2O$ (**2**) with $x \approx 4.5$, is prepared from the reaction of $CsVO_3$:1,3-diaminopropane:H_3PO_4:H_2O

(18) Meier, W. M.; Olson, D. H. *Atlas of Zeolite Structure Types*; American Chemical Society: Washington, DC, 1989.
(19) Wagner, M. J.; Dye, J. L. *J. Solid State Chem.*, in press.

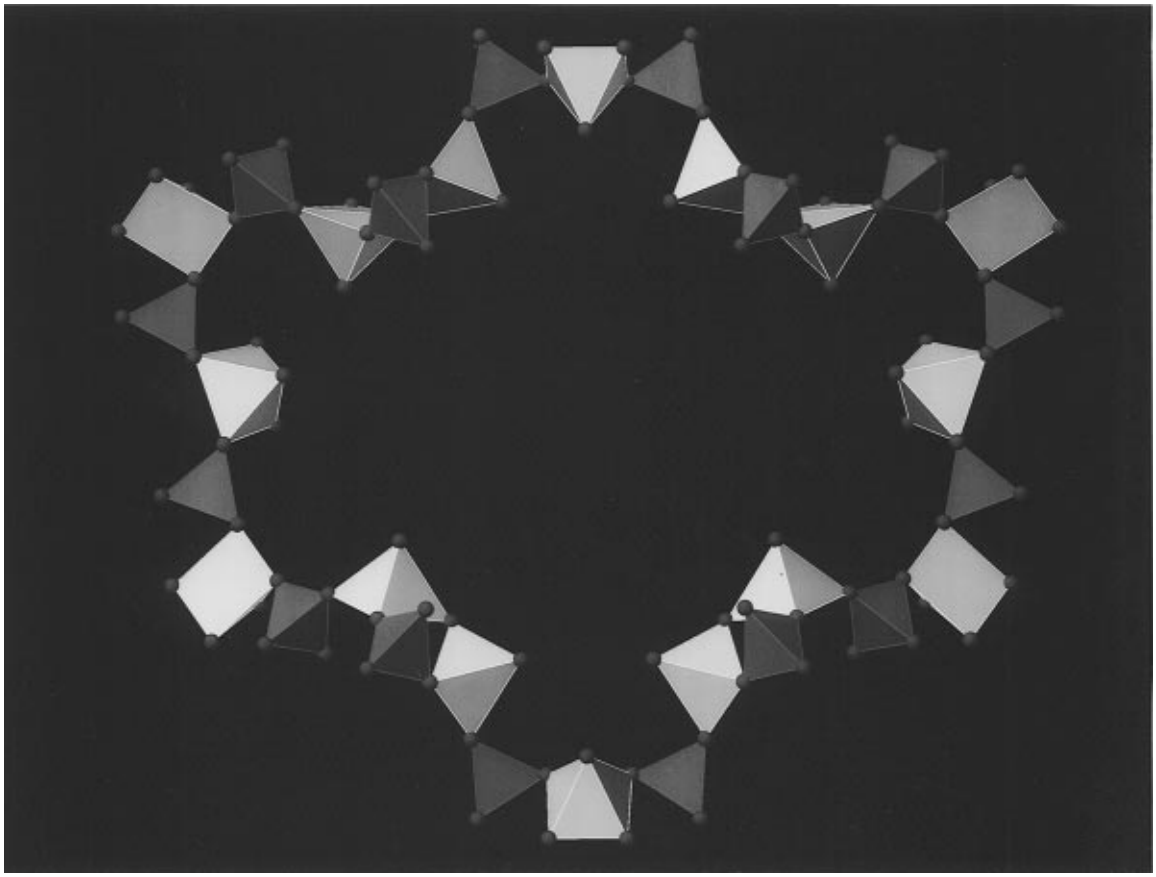

Figure 4. Cross-sectional view, perpendicular to one of the ⟨110⟩ directions, of the 32-ring central section of the large cavity in **1**.

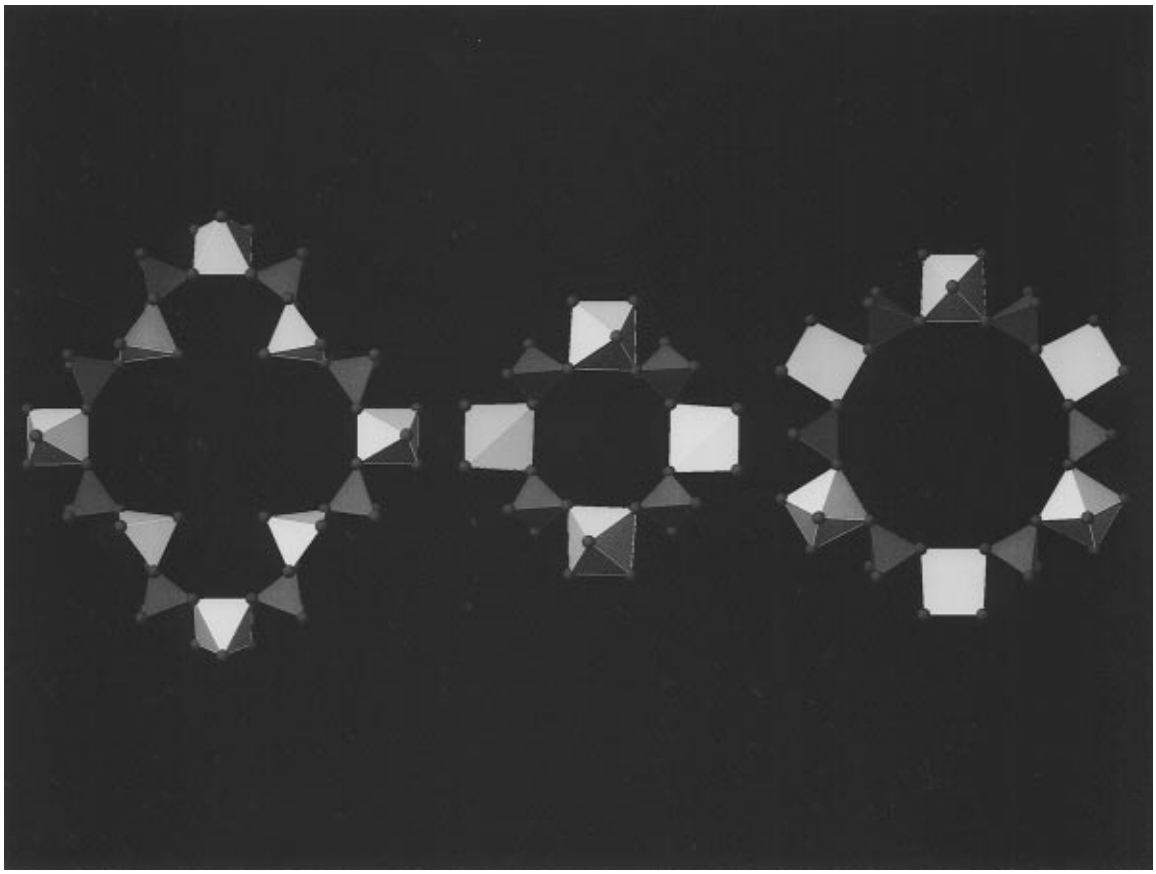

Figure 5. (a) One of the six rectangular 16-ring windows, with free diameters of about 9.4 by 4.4 Å, exiting the large cavity in **1**; (b) the 8-ring window, containing a K^+ cation, present in the small cavity in **1**; (c) one of four 12-ring apertures in each large cavity in **2**.

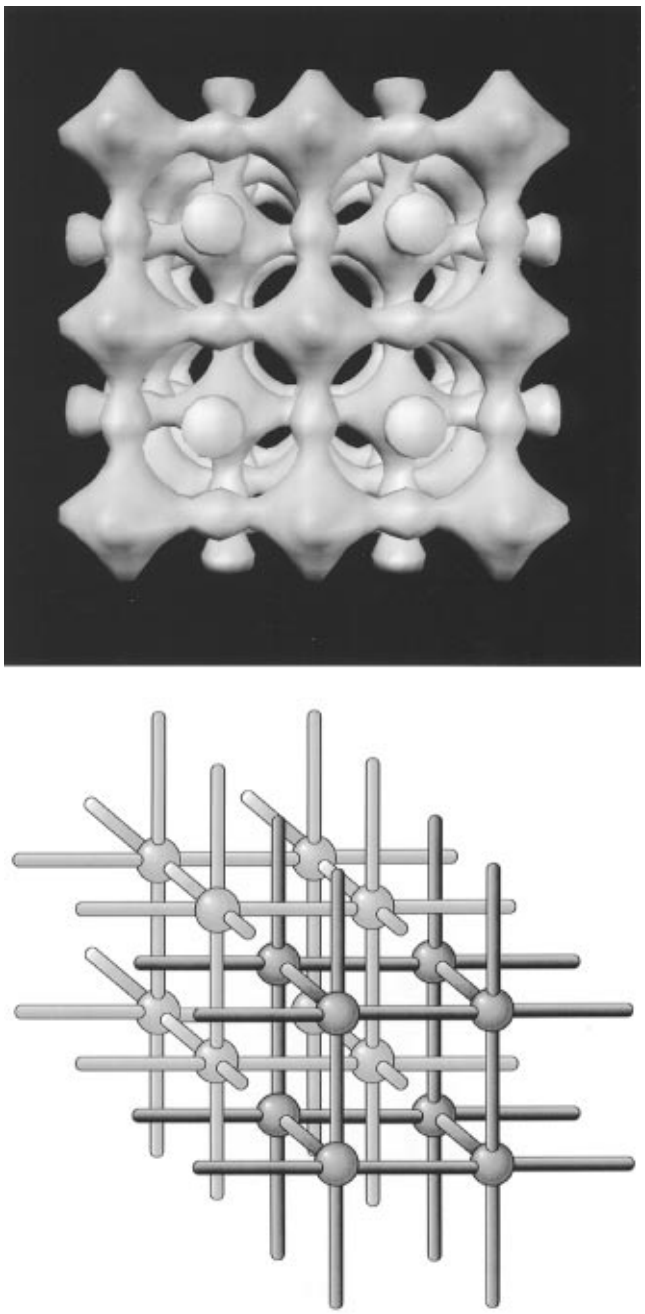

Figure 6. (a, top) A view down [100] of the isosurface (1.6-Å from the van der Waal radius) representing the tunnel structure in **1** along with a schematic representation (b, bottom). There are two crystallographically identical sets of tunnels (related by the body centering of the unit cell) that interpenetrate one another but never intersect.

in a molar ratio of 3:5:5:2000 at 200 °C for 2 days and is isolated in 20% yield (based on V) as green-black cubes (about 5% of the isolated product is a brown solid that contains no V or P). Despite the essential requirement of the propanediamine in the reaction mixture, there is no indication from either the X-ray structure or elemental analysis (found: 0.54% C and <0.1% N) that any organic cation was occluded and the voids are filled with Cs^+ and water molecules only.

(20) Heating a mixture of KVO_3, piperidine, diethylamine, phenylphosphonic acid, phosphoric acid and water in a molar ratio of 1:3:2:1:2:100 at 170 °C for 8 days gives a 30% yield of **3**. The product is contaminated by <5% of an amorphous brown impurity that does not contain V, K, or P.

The framework of phosphate **2** is built up from the same pentamers as found in **1** (Figure 1) but with an entirely different inter pentamer connectivity. Valence sum calculations indicate a total charge of 20.9+ for the five V atoms (average $V^{4.2+}$) which gives a charge on the framework of −3.1 per formula unit agreeing well with the charge of 3+ provided by the three Cs^+ cations. A projection of the unit cell contents of **2**, which crystallizes in the high-symmetry cubic space group $Fd\bar{3}m$, is shown in Figure 2b. As in **1**, there are large and small voids within the framework both of which are surrounded by six V_5 pentamers that occupy positions corresponding to the face centers of a cube, with the V═O bond of the central V atoms in each pentamer lying on the lines that pass through the center of the cube and the midpoint of each face. The six pentamers are bridged together by portions of additional pentamers via interposing phosphate tetrahedra. The large and small cavities differ in the orientation of the pentamer by having either all six pentamers curved outward or all six inward, i.e., the central V═O group oriented toward the interior or exterior of the cavity. When the six V_5 units are oriented outward, a very large cubic shaped cavity results with a minimum free diameter of approximately 14.3 Å and a body diagonal of 20 Å, as shown in Figure 7a. The large cavities are connected to four neighboring cavities in a tetrahedral fashion with a topology identical to carbon atoms in diamond, consistent with the fact that diamond and **2** both crystallize in space group $Fd\bar{3}m$. Each supercage is fused to four adjacent supercages via a 12-ring window (maximum free diameter of 7.3 Å) the plane of which lies perpendicular to the ⟨111⟩ directions as shown in Figure 7c. The manner in which the Cs^+ cations are distributed within the void is shown in Figure 7c. Thus there is a free path through a given supercage (and through the entire structure) defined by two of the 12-ring windows along a ⟨110⟩ direction (Figure 7d) as well as a second free path at 90° to this one. An isosurface representation of the large cavities and their connections to one another is shown in Figure 8 where the resemblance to diamond is obvious. There are an equal number of smaller cubic cavities, with the central V═O of each of the six pentamers oriented toward the interior of the cavity, that have free diameters between opposite V═O oxygens atoms of 5.3 Å. The manner in which the pentamers connect to form the large and small cages, as well as the way the cages connect to form the 3-D lattice, can be understood by examination of the schematic illustration of the lattice in Figure 9.

Preliminary experiments indicate that the frameworks found in both **1** and **2** are relatively defect free and will readily undergo ion-exchange reactions. For example, stirring **3** with a concentrated aqueous solution of either barium or ammonium chloride, conditions that will eventually cause dissolution of the compound, results in complete ion exchange within 2 h according to electron microprobe and infrared absorption measurements. Water vapor absorption isotherms (Figure 10) indicate that both **1** and **2** are capable of sorbing large amounts of this gas. Phosphate **2** displays a type I absorption isotherm[21] and takes up approximately 10 wt % water vapor. For the formula $Cs_3[V_5O_9(PO_4)_2]\cdot$

(21) Ruthven, D. M. *Principles of Adsorption and Adsorption Processes*; John Wiley & Sons: New York, 1984.

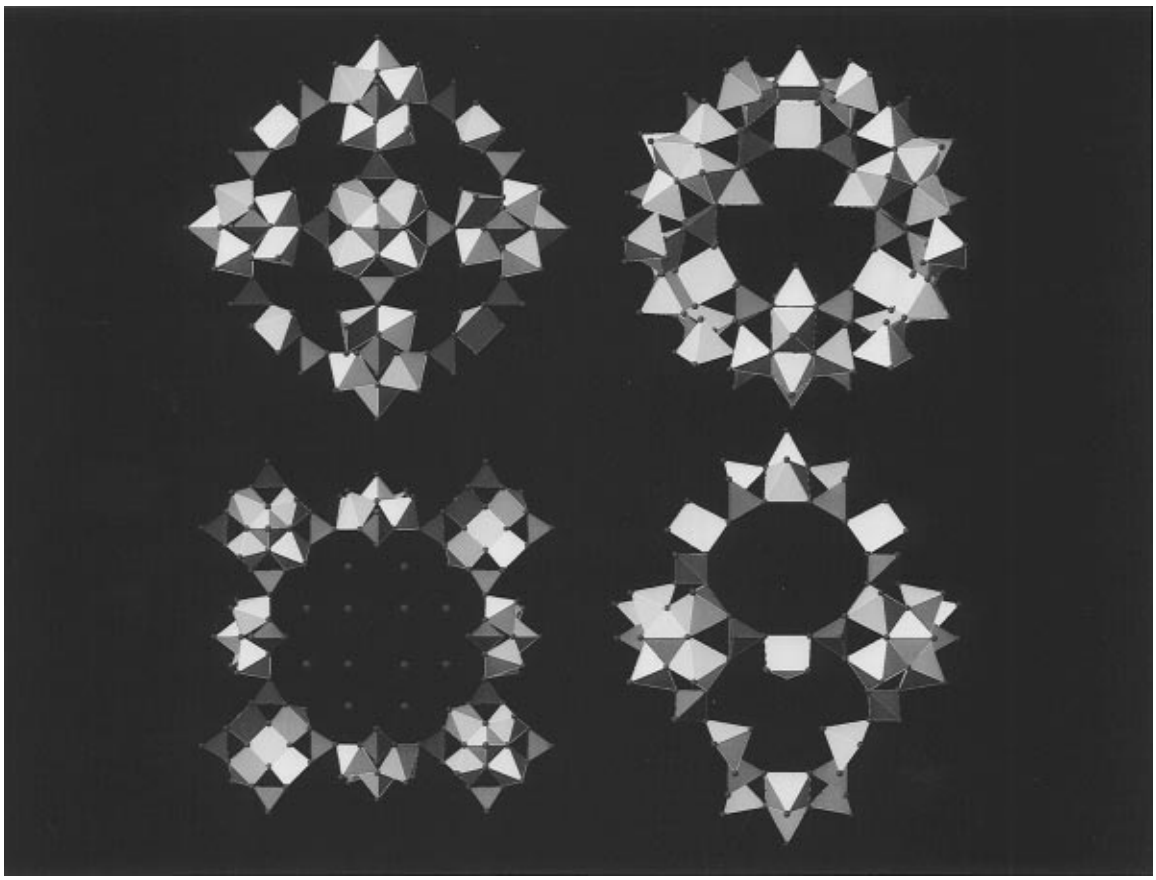

Figure 7. Polyhedral representations of the supercage in phosphate **2**. (a, top left) View of the cage parallel to [100] with the six pentamers lying on the six faces of a cube (the central pentamer obscures the sixth one below it); (b, top right) view of the supercage parallel to [111] through the 12-ring window (foreground) and showing the three V═O groups on the opposite side of the cavity; (c, bottom left) view parallel to [100] showing the 24-ring composed of four of the six pentamers that define the large supercage (the pentamers above and below the plane of the paper have been removed for clarity) and the manner in which the Cs^+ cations order in the cavity; (d, bottom right) a view of the cavity parallel to one of the ⟨110⟩ directions.

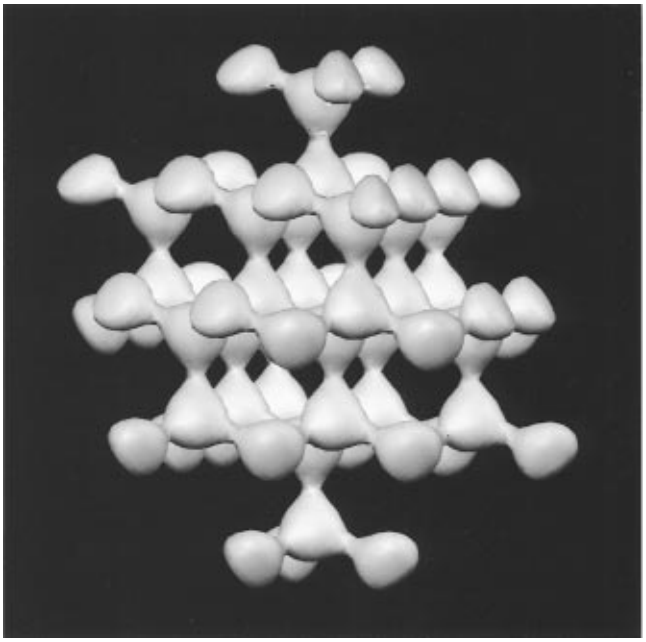

Figure 8. Isosurface representation of the interconnection of the supercages in **2**. The large cavities form a network with a topology identical to the carbon−carbon bonds in diamond, which also crystallizes in space group $Fd\bar{3}m$.

$x H_2O$, a value of 4.5 obtained from the X-ray data is in good agreement with the value obtained from the sorption measurements. The sorptive behavior of Ba^{2+}-

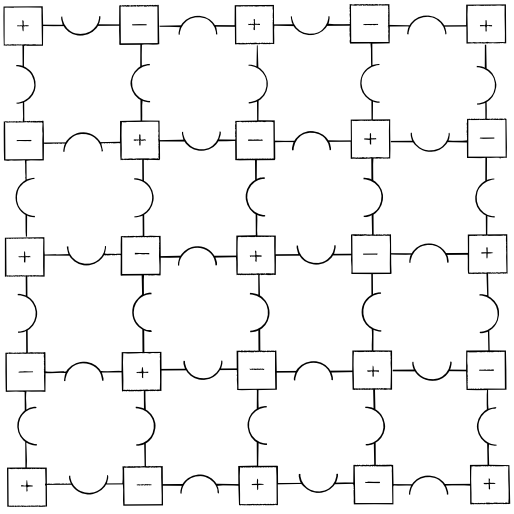

Figure 9. Schematic illustration for the construction of phosphate **2**, where "+" represents a V_5 pentamer curved toward, and "−" curved away from, the plane of the page and the arcs represent the direction of curvature for the pentamers viewed edge on. The structure of **2** is generated by stacking these "layers" in the proper registry and sequence such that the translational repeat corresponding to the unit cell would occur after every four layers. For **2**, the layers would be stacked such that each "+" would be directly over a "−", but with a void from an intervening layer between, and all pentamers viewed edge on are related to the ones directly above and below it by a 4_1 screw axis as required by the space group symmetry.

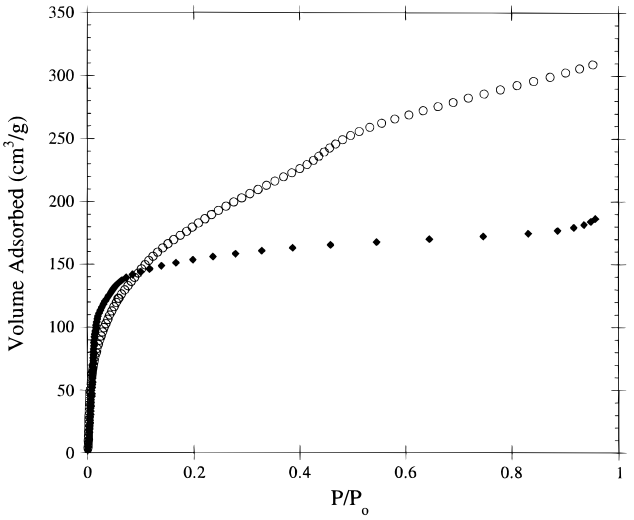

Figure 10. Water vapor absorption isotherm for **2** (diamonds) and Ba^{2+}-exchanged (**3**) after degassing at 50 °C under vacuum. The cm^3 of water vapor are normalized to STP (760 Torr and 273 K).

exchanged **1** is more complicated (Figure 10), but much larger amounts of gas are adsorbed. Experiments with other sorbates are currently underway.

Conclusions

These results show that it is possible to prepare structurally complex open-framework vanadium phosphates possessing cavity sizes, limiting apertures, porosities, and framework densities rivaling those of the most open zeolites and aluminophosphates. The approach used here to synthesize the vanadium phosphate supercage materials depends on achieving reaction conditions under which a building block is formed that cannot form a closed structure with itself on small length scales, in this case the curved $\{V_5O_9(PO_4)_{4/2}\}$ unit. Since the same building block can be utilized in the presence of different cations which serve to direct the conformation of the isocompositional polymerizing 3-D networks, it may be possible to hydrothermally assemble a 3-D covalent oxide in a rational fashion employing this approach. In addition to providing new insight into the fundamental aspects of the hydrothermally mediated self-assembly of inorganic three-dimensional framework materials, the facile preparation of solids containing voids in the 5−25 Å length scale, with cavity walls containing potentially calalytically, magnetically, or photochemically reactive d-block elements in close proximity to the void, could provide new possibilities for molecular recognition and reaction selectivity in solid-state materials.

Acknowledgment. We are grateful to Mr. Tibor Nagy and Dr. Gregor Overney for program development. The work at Syracuse University was supported by NSF Grant CHE 9318824. The work at Michigan State University was supported by the MSU Center for Fundamental Materials Research and by NSF Grant DMR 9402016.

Supporting Information Available: Complete tables of crystallographic conditions, atomic positional parameters, bond lengths and angles, and anisotropic temperature factors for **1** and **2** (15 pages); observed and calculated structure factors (10 pages). Ordering information is given on any current masthead page.

CM950249T